Acta Neuropsychiatrica 2009: 21: 67–74

DOI: 10.1111/j.1601-5215.2009.00361.x

ACTA NEUROPSYCHIATRICA

Rey Visual Design Learning Test performance correlates with white matter structure

Begré S, Kiefer C, von Känel R, Frommer A, Federspiel A. Rey Visual Design Learning Test performance correlates with white matter structure.

Objective: Studies exploring relation of visual memory to white matter are extensively lacking. The Rey Visual Design Learning Test (RVDLT) is an elementary motion, colour and word independent visual memory test. It avoids a significant contribution from as many additional higher order visual brain functions as possible to visual performance, such as three-dimensional, colour, motion or word-dependent brain operations. Based on previous results, we hypothesised that test performance would be related with white matter of dorsal hippocampal commissure, corpus callosum, posterior cingulate, superior longitudinal fascicle and internal capsule.
Methods: In 14 healthy subjects, we measured intervoxel coherence (IC) by diffusion tensor imaging as an indication of connectivity and visual memory performance measured by the RVDLT. IC considers the orientation of the adjacent voxels and has a better signal-to-noise ratio than the commonly used fractional anisotropy index.
Results: Using voxelwise linear regression analyses of the IC values, we found a significant and direct relationship between 11 clusters and visual memory test performance. The fact that memory performance correlated with white matter structure in left and right dorsal hippocampal commissure, left and right posterior cingulate, right callosal splenium, left and right superior longitudinal fascicle, right medial orbitofrontal region, left anterior cingulate, and left and right anterior limb of internal capsule emphasises our hypothesis.
Conclusion: Our observations in healthy subjects suggest that individual differences in brain function related to the performance of a task of higher cognitive demands might partially be associated with structural variation of white matter regions.

Stefan Begré[1], Claus Kiefer[2], Roland von Känel[1], Angela Frommer[3], Andrea Federspiel[3]

[1]Division of Psychosomatic Medicine, Department of General Internal Medicine and [2]Department of Neuroradiology, Inselspital, Bern University Hospital, Bern, Switzerland; and [3]Department of Psychiatric Neurophysiology, University Hospital of Psychiatry, Bern, Switzerland

Keywords: diffusion tensor imaging; healthy; memory; Rey Visual Design Learning Test; white matter

Stefan Begré, MD, Division of Psychosomatic Medicine, Department of General Internal Medicine, Inselspital, Bern University Hospital, CH-3010 Berne, Switzerland.
Tel: +41 31 632 83 61;
Fax: +41 31 382 11 84;
E-mail: stefan.begre@insel.ch

Introduction

The assessment of visual memory is one way to examine memory performance. The Rey Visual Design Learning Test (RVDLT) is an elementary motion, colour- and word-independent visual memory test that consists of 15 abstract, black-and-white-lined, straightforward, two-dimensional figures (1). Subjects are required to memorise the figures in five stages. The number of recalled figures counts for the performance.

Anatomical disconnection between brain regions that underpin different aspects of memory function may produce different patterns of memory disturbance (2–7). Diffusion tensor imaging (DTI) is a relatively novel means of assessing tissue structure providing information about white matter structure. DTI measures diffusion of water molecules in three dimensions. Diffusion of water perpendicular to the direction of the axons is restricted by the myelin sheath and cell membrane such as that the diffusion will be greater along the length of the axon than perpendicular to the axon. Thus, DTI measures diffusion-driven displacements of molecules during their random path along axonal fibres, expressed as fractional anisotropy (FA) or intervoxel coherence (IC) ranging from 0 (isotropic medium) to 1 (fully anisotropic medium). FA is a measure that quantifies the

degree to which diffusion differs in the three dimensions. IC considers the degree of collinearity between the diffusion tensor of the reference voxel and the adjacent voxels, and, moreover, yields a better signal-to-noise ratio than the commonly used FA (8,9). Hence, based on the determination of the similarity of orientation of adjacent voxels, IC reflects a measure of connectivity, expressing fibre coherence at the voxel level with a spatial sampling limited by voxel size. The relation between diffusivity of water molecules in human tissue expressed by anisotropy indices and clinical symptoms was verified post-mortem. Myelin content and axonal density strongly correlated with diffusion anisotropy (10).

A relationship between anisotropy measured by DTI and cognitive function has been shown in healthy people as well as in patients. Individual differences in reaction time performance of a visual choice-paced reaction time test (CRT) in healthy subjects were associated with variations in the white matter underlying the visuospatial attention network; this suggests that increased anisotropy would be a manifestation of faster nerve conduction velocity leading to faster RT (11). White matter anisotropy decreased linearly with increasing age and directly correlated with executive function assessed by the Trail Making Test (12). Reading scores in reading-impaired adults and their control group were significantly directly correlated with white matter diffusion anisotropy (13). Alcoholics had lower regional FA and IC than controls, and a positive association between anisotropy and working memory and attention was also found in alcoholics compared with controls (14). In addition, there was a relationship between FA values and mini-mental state examination (MMSE) scores in Alzheimer's disease (15). Verbal memory performance directly correlated significantly with posterior cingulate bundle anisotropy in Alzheimer's disease and minimal brain impairment and in healthy subjects (16). FA was positively associated with verbal declarative memory in patients suffering from schizophrenia (17). FA values for the splenium of corpus callosum were significantly reduced in patients infected with human immunodeficiency virus and correlated with dementia severity (18). Taken together, a positive correlation between anisotropy and most cognitive measures was shown suggesting that higher cognitive performance is related to biological factors (myelination, fibre density and tissue organisation) that underpin measures such as FA and IC.

The previous findings on a relationship between white matter structure detected by diffusion tensor imaging and cognitive function in neuropsychiatric diseases and healthy people imply that visual memory performance may be associated with white matter structure (11,19,20). As far as we know, however, there is only one study examining visual memory and white matter anisotropy in healthy subjects (21). In the latter study, Begré et al. found a structural difference in white matter between healthy subjects performing low vs. high on the RVDLT, observation of which provided *in vivo* evidence for the contribution of white matter structure to visual memory.

The present study was designed to test the hypothesis whether interindividual differences in visual memory performance (expressed as number of recalled figures in the RVDLT) may be related to interindividual differences in white matter connectivity (expressed as IC). Based on previous results, we specifically hypothesised that visual memory performance would directly be correlated with IC in the dorsal hippocampal commissure (22,23), the corpus callosum (24–26), the posterior cingulate (27), the superior longitudinal fascicle (28) and the internal capsule (29) supporting the notion that all of these brain areas would be involved in visual memory processing.

Material and methods

Subjects

Fourteen right-handed healthy volunteers with no history of major medical, neurological or psychiatric disease were recruited. The study protocol was approved by the local ethics committee (Table 1) and all subjects provided written informed consent. Subjects were instructed to relax and to keep their head still in the magnetic resonance imaging (MRI) scanner. Head motion was minimised with restraining foam pads.

Methods

Performance of the RVDLT. The examiner presented 15 geometric stimulus cards (10 × 7 cm) in a row for 2 s each. After all cards had been presented, the subject was asked to draw all the

Table 1. Subject characteristics

Number	14
Age mean ± SD, years	22.0 ± 3.6
Gender*	Five women; nine men
Intelligence ± SD	111.8 ± 12.4
Performance mean ± SD; variance	11.5 ± 3.8; 14.6

*Not significant considering age, intelligence, and performance ($p < 0.05$, Mann–Whitney).

https://doi.org/10.1111/j.1601-5215.2009.00361.x Published online by Cambridge University Press

designs he or she could recall. For the first recall, the subject had 60 s to draw the designs before the examiner removed the recall sheet. This procedure was repeated until five successive trials with different recall sheets had been completed. For the last four trials, the time allowed for the drawings was 90 s. Eventually, 45 min after completion of the last trial, subjects were asked to redraw from memory as many of the 15 figures as possible. The number of accurately drawn figures was added up to a performance score ranging from 0 to 15 points.

MRI and DTI recording. MRI was performed on a 1.5-Tesla standard clinical MRI scanner (Siemens Vision, Erlangen, Germany) using the standard radiofrequency head coil. A high-resolution three-dimensional (3-D) data set covering the whole brain was collected for each subject through a 3-D magnetisation prepared rapid acquisition gradient echo (MP-RAGE) sequence. Totally 192 slices were accumulated [repetition time (TR) = 6 s, echo time (TE) = 95 ms, matrix size = 256 × 256 voxels, field of view (FOV) = 256 mm, voxel dimension = 1.0 × 1.0 × 1.0 mm]. For diffusion-weighted imaging, a single shot spin-echo echo-planar imaging (SE-EPI) sequence was acquired in the same session. The imaging parameters of the single-shot SE-EPI sequence were defined as follows: matrix size = 96 × 128 voxels, TE = 112 ms, FOV = 240 × 240 mm^2, slice thickness = 5 mm, 12 axial continuous slices, TR = 3 s, pixel bandwidth = 125 kHz, and use of standard head coil and head neck standard shimming. Gradient amplitudes and duration were set to enable detection of tissue-dependent diffusion coefficients by the signal attenuation: G = 22 mT/m, duration TE = 0 ms, intergradient time interval = 40 ms. The diffusion sensitising gradients were applied simultaneously on two axes around the 180° pulse at b = 1800 s/mm^2/axis along six noncollinear directions: (Gx, Gy, Gz) = [(1, 0, 1), (1, 0, −1), (0, 1, 1), (0, 1, −1), (1, 1, 0), (−1, 1, 0)]. This gradient scheme was chosen to minimise acquisition time despite suggestions that the optimal gradient scheme may include more than six gradient directions (30,31). Additionally, one image was acquired with no gradients applied. The calculation and diagonalisation of the diffusion tensor were based on the multivariate regression approach (32). Eddy current corrections were included. Six independent elements of the diffusion tensor were extracted (33). Eigenvalues (magnitude) and eigenvectors (direction) were determined for each voxel, and the IC maps were constructed using the average of the angle between the eigenvector of the largest eigenvalue of a given voxel and its neighbours that represents the extent to which the vectors point the same direction and are, therefore, coherent (8). For each subject, these maps were manually co-registered with the 3-D anatomical maps and, thereafter, spatially normalised in the Talairach space (34) by affine transformation implemented in the BrainVoyager software package. During this co-registration, the voxel dimension of the IC maps was interpolated to 1.0 × 1.0 1.0 mm.

Statistical analysis

Analyses of the images were blinded to visual memory performance. Images were smoothed using a Gaussian filter with a full width at half maximum (FWHM) of 7.5 mm. Automatic segmentation of the 3-D anatomical images (MP-RAGE) for each subject yielded individual probability maps ($p < 0.01$) for grey and white matter (BrainVoyager QX 1.7; Brain Innovation, Maastricht, the Netherlands). The individual 3-D white matter maps were used to compute the largest possible 3-D white matter template (Fig. 1).

In a first step, voxelwise analyses of the IC values were conducted using linear regression analyses to obtain the pattern of correlation with the performance of each subject in the RVDLT. This correlation pattern was computed for DTI voxels within the 3-D white matter template only. The estimation of the correlation was performed using MATLAB programs (MATLAB version 6, release 13; The MathWorks, Inc., Natick, MA, USA). Areas of significant correlation were identified at the cluster level for the threshold $p < 0.01$. Regions of interest based on correlation clusters were generated by using BrainVoyager. To identify volume-corrected regions, clusters were defined as 60 or more neighbouring voxels (60 mm^3) ($p < 0.05$). For each cluster, IC values in the clusters were averaged and tabulated, and Talairach coordinates (34) of the centres of gravity were noted. Clusters were assigned to the underlying white matter using 3-D anatomical data. Location in the brain was selected by both a macroscopic (35) and a microscopic atlas (36), both indicating Talairach coordinates.

In a second step, these significant clusters were further analysed using a general linear model (GLM) that allows population inference. We assumed in this model that RVDLT was the only predictor for IC response. To test for non-normality of the residuals, the Shapiro–Wilk test was computed for each voxel of each cluster. With the Shapiro–Wilk test, the null hypothesis is that residuals follow a normal distribution, i.e. if the p-value is greater than alpha value of 0.05, the null

https://doi.org/10.1111/j.1601-5215.2009.00361.x Published online by Cambridge University Press

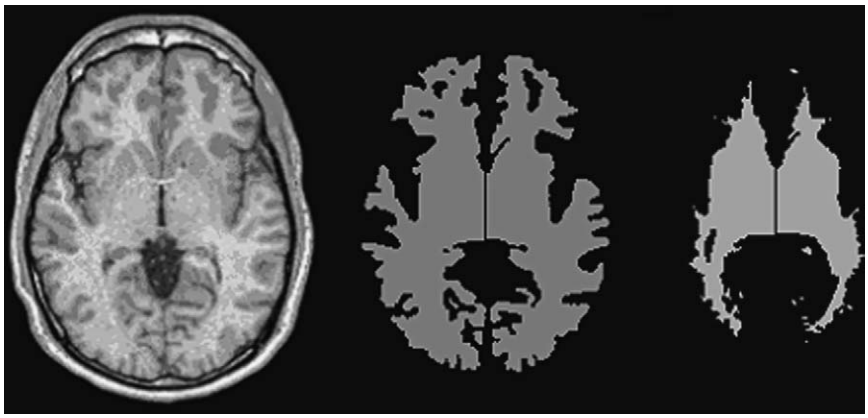

Fig. 1. Representative axial slice in Talairach space of one subject (left), its segmented white matter map (middle), and the largest possible white matter mask including all white matter maps of all subjects (right). To test for correlation of IC values with performance of each subject in the RVDLT, the 3-D segmented white matter maps were used to construct the largest possible white matter mask.

hypothesis will not be rejected (31). Finally, the explained variances of the GLM model were expressed by the R-Square value.

Results

There were no gender differences in terms of age, intelligence, visual memory performance and IC (non-parametric; $p < 0.05$). IQ was strongly related to test performance suggesting that higher estimates of intelligence were associated with better performance in visual memory (Pearson's $r = 0.72$, $df = 12$, $p < 0.004$) (Table 1).

Eleven clusters showed a significant and direct relationship with visual memory test performance (Table 2). Memory performance correlated positively with white matter structure in left and right dorsal hippocampal commissure, left and right posterior cingulate, right callosal splenium, left and right superior longitudinal fascicle, right medial orbitofrontal region, left anterior cingulate, and left and right anterior limb of internal capsule (Fig. 2).

The correlations between IC cluster values and visual memory test performance maintained significance with IQ as a covariate (all $p < 0.05$).

Discussion

In the present study, we show in 14 healthy subjects that visual memory measured by the RVDLT is related to physiological properties in white matter structure, suggesting that individual differences in visual memory performance may be because of differences in white matter connectivity. In a voxel-based linear regression analysis, we assessed the relationship between brain function and white

Table 2. Clusters with significant correlation between IC and visual memory performance ($p < 0.05$)

Cluster number	Region	Talairach coordinates* x, y, z	Cluster size	IC	*t*†	*p*‡	*R*§	SW¶
1	Dorsal commissure HC	−4.8 ± 2, −35 ± 1.5, 14 ± 1.7	121	0.30 ± 0.13	2.7865	0.0165	0.3929	0.6558
2	Dorsal commissure HC	3.1 ± 1.9, −35 ± 1.2, 15 ± 2.1	120	0.31 ± 0.12	2.9493	0.0122	0.4202	0.7168
3	PCC	−10 ± 1.9, −49 ± 1.3, 25 ± 2	126	0.13 ± 0.05	3.6831	0.0031	0.5306	0.5289
4	PCC	8.1 ± 1.6, −50 ± 1.9, 23 ± 1.7	115	0.15 ± 0.05	3.5604	0.0039	0.5137	0.6051
5	Splenium CC	16 ± 3.8, −27 ± 3.0, 27 ± 0.5	137	0.20 ± 0.06	4.2618	0.0011	0.6022	0.6102
6	SLF	−33 ± 1.2, −25 ± 1.5, 26 ± 1.1	64	0.25 ± 0.07	3.2628	0.0068	0.4701	0.7863
7	SLF	33 ± 1.4, −32 ± 3.6, 27 ± 0.5	63	0.22 ± 0.09	3.0336	0.0104	0.4340	0.7915
8	Medial orbitofrontal	19 ± 1.7, 25 ± 0.9, −2.7 ± 1.9	76	0.24 ± 0.06	3.6421	0.0034	0.5250	0.7111
9	ACC	−9.1 ± 2.2, 30 ± 1.8, 8.7 ± 2.2	105	0.31 ± 0.09	3.2399	0.0071	0.4666	0.7470
10	Internal C anterior limb	−16 ± 3.9, 6 ± 1.1, 1.7 ± 2.7	133	0.19 ± 0.04	3.8387	0.0024	0.5512	0.9416
11	Internal C anterior limb	15 ± 1.3, 7.3 ± 1.6, 4.5 ± 2.0	96	0.25 ± 0.06	3.2347	0.0072	0.4658	0.5714

ACC, anterior cingulate cortex; C, capsule; CC, corpus callosum; HC, hippocampus; PCC, posterior cingulate cortex; SLF, superior longitudinal fascicle.
*Positive *x*-coordinates are in the right, negative *x*-coordinates in the left hemisphere.
†*T*-value of ±random effect GLM with model assuming that RVDLT was the only predictor for IC response.
‡p = exact level of significance of correlation.
§Explained Variance derived from R-Square in GLM.
¶Shapiro–Wilk test for non-normality of the residuals.

https://doi.org/10.1111/j.1601-5215.2009.00361.x Published online by Cambridge University Press

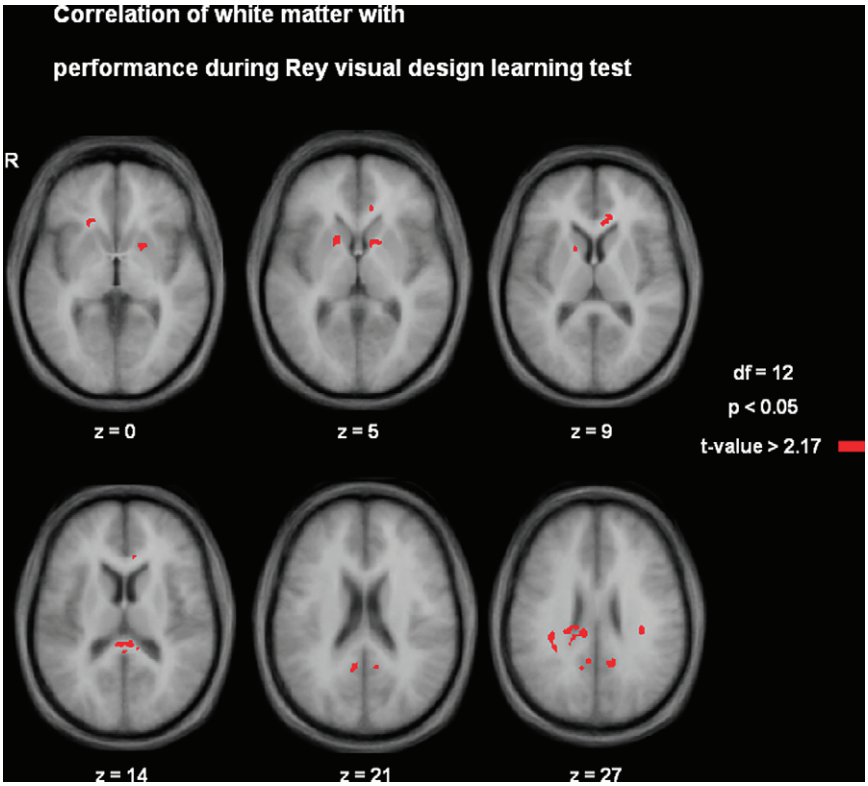

Fig. 2. Axial slices of a representative subject showing the locations of statistically significant correlations of white matter with performance ($p < 0.05$). Numbers assigned to each slice indicate the *z*-coordinate in Talairach space.

matter connectivity by means of the intervoxel anisotropy index (IC) and with visual memory performance. We observed that performance correlated with white matter structure of the left and right dorsal hippocampal commissure, the left and right posterior cingulate, the right callosal splenium, the left and right superior longitudinal fascicle, the right medial orbitofrontal region, the left anterior cingulate and the left and right anterior limb of internal capsule.

Most commonly used visual learning test paradigms imply 3-D, colour, motion or word-dependent brain operations. We chose the RVDLT as a straightforward visual learning paradigm, using elementary, geometric, black-and-white-lined figures. This design avoids a significant contribution from as many additional higher order visual brain functions as possible to visual performance.

Supporting our hypothesis and corroborating previous studies showing a relationship between anisotropy measured by DTI and memory performance in memory-affected patients (2,12,13,37–40), and in healthy subjects (41), visual memory performance was positively correlated with white matter structure in 11 definite brain regions. This observation suggests that the less connectivity in the white matter bundles in these regions, the poorer the memory performance on the one hand, and that the more connectivity structure shown in the white matter bundles in these clusters, the better the memory performance on the other. Therefore, we suggest that, in brain regions where memory performance is correlated with IC, the white matter bundles support processing RVDLT. The fact that we did not find any statistical association with RVDLT performance in the clusters representing correlation of IC with RVDLT performance (data not shown) in a cancellation test requiring visual scanning (d2 test) (1) supports our interpretation. We therefore may state that the clusters of white matter regions were mainly independent of processing of visual scanning but instead related to neuron bundles involved in the task. Hence, we may assume that significant voxel clusters are structural correlates of specifically visual memory capacity. Incomplete myelination in general, associated with white matter changes, may lead to slower information processing, aberrant neuronal signalling, and, therefore, lower task performance. Accordingly, the more efficient the regional myelination, the faster the information processing on this site, and, eventually, the higher the task performance (1,18,42). In other words, individual structural differences may lead to

https://doi.org/10.1111/j.1601-5215.2009.00361.x Published online by Cambridge University Press

different functionality (2,5,37,41,43–45). Corroborating the previous literature about anisotropy in neuropsychiatric diseases and healthy people, we detected a positive association between anisotropy values and brain function (2,18–20,41).

The finding of clusters was expected within white matter of the dorsal hippocampal commissure, the corpus callosum, the posterior cingulate, the superior longitudinal fascicle and the internal capsule. A potentially important cluster was found in the dorsal hippocampal commissure where fibres travel between the splenium and the hippocampal formation. Based on previous studies in humans (22,46), the dorsal hippocampal commissure is supposed to be important for memory function. The hippocampus is activated during retrieval of mental images (23). The posterior part of the corpus callosum plays a predominant role in the right–left transfer of spatial information guiding constructional performance (23). As previously shown, impairment of the posterior part of the corpus callosum leads to derogation of human visual memory (25,26). The posterior cingulate cortex was suggested to support visual recall performance (27). An interplay between different neurofunctional systems is important in memory and learning (47,48). The major association pathway that links the frontal lobe with the parietal cortex is the superior longitudinal fascicle (28). Almost all neural traffic to and from the cerebral cortex passes through the internal capsule (29).

Furthermore, we found two clusters in the orbitofrontal region and the anterior cingulate, respectively. The orbitofrontal region plays an important role in encoding abstract visual information (49). The anterior cingulate cortex seems to be involved if an effort is needed to carry out a task such as early learning and problem solving (50), is implicated in reinforcement-guided decision making and error detection (51) and is responsible for rendering new memories permanent (52).

We mention three important limitations of our findings. Firstly, even if acquisition time can be reduced by applying a DTI sequence with a minimum of tensor directions, other advanced acquisition techniques might improve accuracy of measurements. Therefore, future studies should further enhance signal-to-noise ratio by image averaging of a sequence with more tensor directions. Secondly, the physical mechanisms involved in the diffusion anisotropy in white matter are not fully understood. Some authors feel that the diffusion barriers presented by the cell membrane and myelin sheath play a significant role (53). However, IC provides only an indirect maker of white matter structural properties. Thirdly, although there is good clinical and experimental evidence for an association between DTI and cognitive performance in healthy individuals and in patient populations (2,54), the *a priori* assumption that the diffusion of water molecules along axonal bundles can be used as a measure of neural connectivity is, as yet, unproven. Therefore, whether differences in IC between subjects in our study relate to interconnections between neural networks in individuals with different visual learning skills, remains open.

Bearing these limitations in mind, our study suggests *in vivo* evidence for a contribution of white matter physiological properties to the recall of visual memory in healthy people. DTI could be a promising tool to help to better understand the interconnecting neurofunctional network of visual processing and its impact on clinical behaviour. Based on our findings, further studies combining DTI fibre tracking with functional methods seem a guarantee to learn more about behavioural consequences of structural brain conditions.

Acknowledgements

We thank Regula Schweizer for performing the magnetic resonance imaging measurements and Annette Kocher for proofreading the manuscript.

References

1. Spreen O, Strauss E. A compendium of neuropsychological tests: administration, norms and commentary, New York: Oxford University Press, 1991.
2. Begré S, Federspiel A, Kiefer C, Schroth G, Strik WK, Dierks T. Alterations of white matter connectivity in first episode schizophrenia. Neurobiol Dis 2006;**22**:702–709.
3. Nobili F, Brugnolo A, Calvini P et al. Resting SPECT-neuropsychology correlation in very mild Alzheimer's disease. Clin Neurophysiol 2005;**116**:364–375.
4. Cohen L, Henry C, Dehaene S et al. The pathophysiology of letter-by-letter reading. Neuropsychologia 2004; **42**:1768–1780.
5. Begré S, Federspiel A, Kiefer C, Schroth G, Dierks T, Strik WK. Reduced hippocampal anisotropy related to anteriorization of alpha EEG in schizophrenia. Neuroreport 2003;**14**:739–742.
6. Schmidtke K, Manner H, Kaufmann R, Schmolck H. Cognitive procedural learning in patients with frontostriatal lesions. Learn Mem 2002;**9**:419–429.
7. Dimond SJ, Scammell RE, Brouwers EY, Weeks R. Functions of the centre section (trunk) of the corpus callosum in man. Brain 1977;**100**:543–562.
8. Pierpaoli C, Basser PJ. Toward a quantitative assessment of diffusion anisotropy. Magn Reson Med 1996;**36**:893–906.
9. Skare S, Li T, Nordell B, Ingvar M. Noise considerations in the determination of diffusion tensor anisotropy. Magn Reson Imaging 2000;**18**:659–669.
10. Mottershead JP, Schmierer K, Clemence M et al. High field MRI correlates of myelin content and axonal density

https://doi.org/10.1111/j.1601-5215.2009.00361.x Published online by Cambridge University Press

in multiple sclerosis – a post-mortem study of the spinal cord. J Neurol 2003;**250**:1293–1301.
11. Tuch DS, Salat DH, Wisco JJ, Zaleta AK, Hevelone ND, Rosas HD. Choice reaction time performance correlates with diffusion anisotropy in white matter pathways supporting visuospatial attention. Proc Natl Acad Sci U S A 2005;**102**:12212–12217.
12. O'Sullivan M, Jones DK, Summers PE, Morris RG, Williams SC, Markus HS. Evidence for cortical "disconnection" as a mechanism of age-related cognitive decline. Neurology 2001;**57**:632–638.
13. Klingberg T, Hedehus M, Temple E et al. Microstructure of temporo-parietal white matter as a basis for reading ability: evidence from diffusion tensor magnetic resonance imaging. Neuron 2000;**25**:493–500.
14. Pfefferbaum A, Sullivan EV, Hedehus M, Lim KO, Adalsteinsson E, Moseley M. Age-related decline in brain white matter anisotropy measured with spatially corrected echo-planar diffusion tensor imaging. Magn Reson Med 2000;**44**:259–268.
15. Sun Y, Du XK, Zhang ZX, Chen X. [Relationship between the data from MR-diffusion tensor imaging and the clinical cognitive evaluation in Alzheimer's disease]. Zhongguo Yi Xue Ke Xue Yuan Xue Bao 2004;**26**:134–138.
16. Fellgiebel A, Muller MJ, Wille P et al. Colour-coded diffusion-tensor-imaging of posterior cingulate fibre tracts in mild cognitive impairment. Neurobiol Aging 2005; **26**:1193–1198.
17. Lim KO, Ardekani BA, Nierenberg J, Butler PD, Javitt DC, Hoptman MJ. Voxelwise correlational analyses of white matter integrity in multiple cognitive domains in schizophrenia. Am J Psychiatry 2006;**163**:2008–2010.
18. Wu Y, Storey P, Cohen BA, Epstein LG, Edelman RR, Ragin AB. Diffusion alterations in corpus callosum of patients with HIV. AJNR Am J Neuroradiol 2006;**27**:656–660.
19. Peters A. The effects of normal aging on myelin and nerve fibres: a review. J Neurocytol 2002;**31**:581–593.
20. Oppenheim C, Rodrigo S, Poupon C et al. [Diffusion tensor MR imaging of the brain. Clinical applications.]. J Radiol 2004;**85**:287–296.
21. Begre S, Frommer A, von Kanel R, Kiefer C, Federspiel A. Relation of white matter anisotropy to visual memory in 17 healthy subjects. Brain Res 2007;**1168**:60–66.
22. Gloor P, Salanova V, Olivier A, Quesney LF. The human dorsal hippocampal commissure. An anatomically identifiable and functional pathway. Brain 1993;**116**(Pt 5): 1249–1273.
23. Ishai A, Haxby JV, Ungerleider LG. Visual imagery of famous faces: effects of memory and attention revealed by fMRI. Neuroimage 2002;**17**:1729–1741.
24. Boldrini P, Zanella R, Cantagallo A, Basaglia N. Partial hemispheric disconnection syndrome of traumatic origin. Cortex 1992;**28**:135–143.
25. Hasegawa I. Neural mechanisms of memory retrieval: role of the prefrontal cortex. Rev Neurosci 2000;**11**:113–125.
26. Alsaadi T, Binder JR, Lazar RM, Doorani T, Mohr JP. Pure topographic disorientation: a distinctive syndrome with varied localization. Neurology 2000;**54**:1864–1866.
27. Berthoz A. Parietal and hippocampal contribution to topokinetic and topographic memory. Philos Trans R Soc Lond B Biol Sci 1997;**352**:1437–1448.
28. Tamura H, Takahashi S, Kurihara N, Yamada S, Hatazawa J, Okudera T. Practical visualization of internal structure of white matter for image interpretation: staining a spin-echo T2-weighted image with three echo-planar diffusion-weighted images. AJNR Am J Neuroradiol 2003;**24**:401–409.
29. Nolte J. The human brain: an introduction to its functional anatomy, 4th edn. St Louis: Mosby, Inc., 1999.
30. Jones DK, Horsfield MA, Simmons A. Optimal strategies for measuring diffusion in anisotropic systems by magnetic resonance imaging. Magn Reson Med 1999;**42**:515–525.
31. Jones DK, Symms MR, Cercignani M, Howard RJ. The effect of filter size on VBM analyses of DT-MRI data. Neuroimage 2005;**26**:546–554.
32. Basser PJ, Pierpaoli C. A simplified method to measure the diffusion tensor from seven MR images. Magn Reson Med 1998;**39**:928–934.
33. Basser PJ, Pierpaoli C. Microstructural and physiological features of tissues elucidated by quantitative-diffusion-tensor MRI. J Magn Reson B 1996;**111**:209–219.
34. Talairach J, Tournoux P. A co-planar stereotactic atlas of the human brain: an approach to cerebral imaging, New York: Thieme Medical publishers Inc., 1988.
35. Nowinsky L, Bryan N, Rhaghavan R. The electronic clinical brain atlas, New York: Thieme Medical Publisher Inc., 2004.
36. May A. The contribution of functional neuroimaging to primary headaches. Neurol Sci 2004;**25**(Suppl 3):S85–S88.
37. Begre S, Koenig T. Cerebral disconnectivity: an early event in schizophrenia. Neuroscientist 2008;**14**:19–45.
38. Takahashi S, Yonezawa H, Takahashi J, Kudo M, Inoue T, Tohgi H. Selective reduction of diffusion anisotropy in white matter of Alzheimer disease brains measured by 3.0 Tesla magnetic resonance imaging. Neurosci Lett 2002;**332**: 45–48.
39. Moseley M, Bammer R, Illes J. Diffusion-tensor imaging of cognitive performance. Brain Cogn 2002;**50**:396–413.
40. Muller MJ, Greverus D, Dellani PR et al. Functional implications of hippocampal volume and diffusivity in mild cognitive impairment. Neuroimage 2005;**28**:1033–1042.
41. Begré S, Frommer A, von Kanel R, Kiefer C, Federspiel A. Relation of white matter anisotropy to visual memory in 17 healthy subjects. Brain Res 2007;**1168**:60–66.
42. Begré S, Federspiel A, Kiefer C, Schroth G, Strik WK, Dierks T. Alterations of white matter connectivity in first episode schizophrenia. Neurobiol Dis 2006;**22**: 702–709.
43. Ridler K, Veijola JM, Tanskanen P et al. Fronto-cerebellar systems are associated with infant motor and adult executive functions in healthy adults but not in schizophrenia. Proc Natl Acad Sci U S A 2006;**103**:15651–15656.
44. Antonova E, Kumari V, Morris R et al. The relationship of structural alterations to cognitive deficits in schizophrenia: a voxel-based morphometry study. Biol Psychiatry 2005;**58**:457–467.
45. Ho BC, Andreasen NC, Nopoulos P, Arndt S, Magnotta V, Flaum M. Progressive structural brain abnormalities and their relationship to clinical outcome: a longitudinal magnetic resonance imaging study early in schizophrenia. Arch Gen Psychiatry 2003;**60**:585–594.
46. Palmini AL, Gloor P, Jones-Gotman M. Pure amnestic seizures in temporal lobe epilepsy. Definition, clinical symptomatology and functional anatomical considerations. Brain 1992;**115**(Pt 3):749–769.
47. Poldrack RA, Rodriguez P. How do memory systems interact? Evidence from human classification learning. Neurobiol Learn Mem 2004;**82**:324–332.
48. Todd JJ, Marois R. Capacity limit of visual short-term memory in human posterior parietal cortex. Nature 2004; **428**:751–754.

https://doi.org/10.1111/j.1601-5215.2009.00361.x Published online by Cambridge University Press

49. Frey S, Petrides M. Orbitofrontal cortex and memory formation. Neuron 2002;**36**:171–176.
50. Allman JM, Hakeem A, Erwin JM, Nimchinsky E, Hof P. The anterior cingulate cortex. The evolution of an interface between emotion and cognition. Ann N Y Acad Sci 2001; **935**:107–117.
51. Rushworth MF, Behrens TE, Rudebeck PH, Walton ME. Contrasting roles for cingulate and orbitofrontal cortex in decisions and social behaviour. Trends Cogn Sci 2007; **11**:168–176.
52. Wiltgen BJ, Brown RA, Talton LE, Silva AJ. New circuits for old memories: the role of the neocortex in consolidation. Neuron 2004;**44**:101–108.
53. Beaulieu C. The basis of anisotropic water diffusion in the nervous system – a technical review. NMR Biomed 2002; **15**:435–455.
54. Grieve SM, Williams LM, Paul RH, Clark CR, Gordon E. Cognitive aging, executive function, and fractional anisotropy: a diffusion tensor MR imaging study. AJNR Am J Neuroradiol 2007;**28**:226–235.

https://doi.org/10.1111/j.1601-5215.2009.00361.x Published online by Cambridge University Press